

# Clinical Relevance of Parafoveal Intercapillary Spaces and Foveal Avascular Zone in Diabetic Retinopathy Without Macular Edema

Noriko Terada, Tomoaki Murakami, Kenji Ishihara, Yoko Dodo, Keiichi Nishikawa, Kentaro Kawai, and Akitaka Tsujikawa

Department of Ophthalmology and Visual Sciences, Kyoto University Graduate School of Medicine, Kyoto, Japan

Correspondence: Tomoaki Murakami, 54 Shougoin Kawahara-cho, Sakyo-ku, Kyoto 606-8507, Japan; [mutomo@kuhp.kyoto-u.ac.jp](mailto:mutomo@kuhp.kyoto-u.ac.jp).

Received: May 31, 2022

Accepted: October 11, 2022

Published: November 2, 2022

Citation: Terada N, Murakami T, Ishihara K, et al. Clinical relevance of parafoveal intercapillary spaces and foveal avascular zone in diabetic retinopathy without macular edema. *Invest Ophthalmol Vis Sci*. 2022;63(12):4. <https://doi.org/10.1167/iovs.63.12.4>

**PURPOSE.** To investigate the clinical significance of intercapillary spaces on swept source optical coherence tomography angiography images in diabetic retinopathy.

**METHODS.** We retrospectively reviewed 110 eyes of 110 patients suffering from diabetic retinopathy without macular edema for whom  $3 \times 3$  mm swept source optical coherence tomography angiography images centered on the fovea were obtained. Automatic image processing of the superficial slab images allowed us to define the areas encircled by retinal vessels as intercapillary spaces within the central 2-mm circle. We evaluated how the quantitative parameters of intercapillary spaces are associated with logMAR and feasible to diagnose diabetic macular ischemia.

**RESULTS.** Total counts ( $\rho = -0.419$ ;  $P < 0.001$ ) rather than morphologic parameters of the intercapillary spaces showed a significant correlation with logMAR. There were individual levels of correlations between logMAR and counts of intercapillary spaces in individual sectors. In particular, the summed numbers of the spaces in three highly significant sectors were more significantly associated with logMAR ( $\rho = -0.515$ ;  $P < 0.001$ ). Multivariate analyses confirmed that the number of the intercapillary spaces ( $\beta = -0.266$ ;  $P = 0.016$ ) and foveal avascular zone area ( $\beta = 0.227$ ;  $P = 0.042$ ) were related to logMAR. The clustering using the foveal avascular zone area and the number of intercapillary spaces revealed two major clusters; one had fewer intercapillary spaces ( $P < 0.001$ ) and poorer logMAR ( $P < 0.001$ ) than the other, with a wide range of the foveal avascular zone area.

**CONCLUSIONS.** Decreased intercapillary spaces contribute to visual impairment in diabetic retinopathy and suggest one possible criterion of objective diagnosis of diabetic macular ischemia.

Keywords: diabetic retinopathy, diabetic macular ischemia, intercapillary space, foveal avascular zone, optical coherence tomography angiography

Diabetic retinopathy (DR) is a leading cause of vision loss in people of working ages worldwide.<sup>1,2</sup> In addition to the morphological changes in retinal vessels, capillary nonperfusion exacerbates retinal neurodegeneration.<sup>3,4</sup> Neuroglial cells exposed to hypoxia secrete VEGF and concomitantly promote angiogenesis and vascular hyperpermeability, which clinically contribute to the pathogenesis in proliferative diabetic retinopathy (PDR) and diabetic macular edema (DME). In the era of anti-VEGF therapy, therapeutic strategies against *diabetic macular ischemia* should be established.<sup>5</sup>

Retinal vessels originate from the optic disc and mainly run within the ganglion cell layer. They bifurcate into the capillaries in the nerve fiber layer and those in the inner and outer borders of the inner nuclear layer.<sup>6</sup> Multiple retinal vascular plexus layers mainly nourish the neurons in inner retinal layers which allow signal transduction. Classically, fluorescein angiography (FA) shows the feasibility of evaluating the foveal avascular zone (FAZ), which enables us to diagnose ischemic maculopathy subjectively.<sup>7</sup>

However, multilayered vascular plexuses and the leakage of fluorescein dye often make it difficult to evaluate three-dimensional vessels in the parafovea or perifovea on FA images. In contrast, optical coherence tomography angiography (OCTA) delineates retinal vessels three-dimensionally and has advantages in the selective assessments of superficial and deep vascular plexuses in any areas of the macula.<sup>8,9</sup> It allows us to quantify perfusion or nonperfusion indices to investigate microcirculatory disturbance.<sup>5</sup>

Comparative studies between structural OCT and OCTA images have revealed the disturbance of the neurovascular unit in DR.<sup>10,11</sup> It has recently been reported that the nonperfused areas (NPAs) in the superficial vascular plexus are accompanied by no boundaries between the nerve fiber layer and ganglion cell layer, and cystoid spaces in the inner nuclear layer often correspond to the NPAs in the deep vascular layer.<sup>11</sup> Previous publications showed a modest association between the FAZ areas and the reduction of visual acuity (VA) in DR, which is consistent with the simultaneous neurovascular degeneration.<sup>12,13</sup> However, there is

a question of whether ischemic changes at the fovea and in the parafovea are critical for bipolar cells and subsequent ganglion cells from foveal cone photoreceptors, respectively, which are centrifugally displaced.<sup>14</sup>

We have recently proposed an intercapillary space spectrum that contains both healthy intercapillary areas and pathophysiological NPAs on OCTA images; this spectrum can be used to evaluate the processes of capillary nonperfusion automatically and objectively.<sup>15</sup> In this study, we investigated whether the characteristics of capillary nonperfusion in the parafovea are associated with VA and the diagnostic significance of diabetic macular ischemia in DR without center-involving DME.

## METHODS

### Participants

In this retrospective study, we reviewed 110 consecutive eyes of 110 patients with DR for whom swept source OCTA images of sufficient quality (signal strength index of 8 or more) were obtained. The inclusion criteria were DR and central  $3 \times 3$  mm swept source OCTA images centered on the fovea had been acquired. We excluded eyes with center-involved DME, severe media opacity, an axial length of less than 22 mm or more than 26 mm, any other chorioretinal disease, other ocular diseases that lead to visual impairment, photocoagulation within 6 months before imaging, previous treatment for macular pathology, cataract surgery within 3 months before imaging, or any intraocular surgery other than cataract surgery. We further excluded eyes that received other treatments for DR or DME than panretinal photocoagulation. Additional exclusion criteria were poor image quality (signal strength index of 7 or less) or severe segmentation error in the superficial slab. If both eyes met these criteria, we selected the right eye for this study. All research and measurements were performed in compliance with the tenets of the Declaration of Helsinki and with the approval of the Kyoto University Graduate School and Faculty of Medicine Ethics Committee. Written informed consent was obtained from all participants.

### Fundus Imaging

We measured the refraction and subsequent best-corrected decimal VA and converted it to the logMAR. After a comprehensive ophthalmic examination, the axial length and the central subfield thickness were measured using partial coherence interferometry (IOL Master, Carl Zeiss Meditec, Inc., Dublin, CA) and Spectralis OCT (Heidelberg Engineering, Heidelberg, Germany), respectively. Eyes with a central subfield thickness of greater than 320  $\mu$ m or 305  $\mu$ m for male or female patients, respectively, were diagnosed as center-involved DME.<sup>16</sup>

Swept source OCTA images within the nominal  $3 \times 3$  mm square centering on the fovea were acquired using Plex Elite 9000 (Carl Zeiss Meditec, Inc.). The nominal  $3 \times 3$  mm square was obtained with  $300 \times 300$  A-scans and digitally converted to a  $1024 \times 1024$  pixel array for quantitative analyses.

### Intercapillary Spaces

Among several perfusion or nonperfusion indices, we selected intercapillary spaces and the FAZ, because we

consistently evaluated the circulation disturbance in both the parafovea and fovea. Several publications have proposed each method to detect NPAs on OCTA images.<sup>17–21</sup> We hypothesized the morphological continuum from healthy intercapillary areas to pathological NPAs and therefore defined areas enclosed by retinal vessels as intercapillary spaces in this study, as proposed recently.<sup>15</sup> Because we considered that the transient and persistent capillary nonperfusion may affect neuronal function, we selected a single en face image, but not the smoothed images.<sup>17,18</sup> Additionally, we focused on the superficial layer, because VA depends on the signals derived from the foveal photoreceptors and transmitted to the bipolar cells and ganglion cells in the superficial slab. All intercapillary spaces were assessed quantitatively on OCTA images according to four steps, as described previously<sup>15</sup>: (1) the construction of the superficial en face OCTA images according to the default settings of the manufacturer's software, (2) the determination of the central 2-mm area using image processing software (Adobe Photoshop, Adobe Systems Inc, San Jose, CA), (3) the binarization of retinal vessels by the Phansalkar adaptive local thresholding method of ImageJ (NIH, Bethesda, MD) (Fig. 1), and (4) quantitative analyses of intercapillary spaces. The Analyze Particles function of ImageJ allowed us to detect each intercapillary space automatically and quantify its geometric parameters (area, perimeter, maximum diameter, and minimum diameter) and the coordinates ( $x, y$ ) of its centroid. The space containing the foveal center was defined as the FAZ. The pixels were converted to millimeters or square millimeters, after the lateral length was corrected for the axial length according to Bennett formula.<sup>22</sup>

In addition to a few morphological parameters, we evaluated the association between logMAR and counts of intercapillary spaces. We further counted the number of intercapillary spaces after size thresholding or within the specific locations. We selected stepwise size thresholds (from 0.01 to 0.05 mm<sup>2</sup>), and evaluated the association between logMAR and the number of intercapillary spaces smaller than each threshold in the central circle with a diameter of 2 mm.

We further assessed the relationship between logMAR and the counts of intercapillary spaces in each sector, which was divided according to the orientation to and distance from the foveal center. We first determined ring 1 (0.375–0.500 mm from the center), ring 2 (0.500–0.625 mm), ring 3 (0.625–0.750 mm), ring 4 (0.750–0.875 mm), and ring 5 (0.875–1.000 mm). Second, we divided a 360° circle into octants of 45° (superior, superonasal, nasal, inferonasal, inferior, inferotemporal, temporal, and superotemporal octants), followed by the creation of 40 sectors in the parafovea. We hypothesized that the centroid of intercapillary spaces represents their location; accordingly, we counted the centroids of intercapillary spaces within each sector. To exclude the false positive in the multiple statistical tests, we further prepared other two annulus patterns, that is, three and four rings in the parafovea, and used the similar analyses.

We quantified three typical perfusion indices, that is, vessel density, vessel length density, and fractal dimension, as described previously.<sup>23</sup> Briefly, the flow signals on the binarized images using the local thresholding was quantified for the vessel density. Subsequent skeletonized vessels were also measured as the vessel length density. The fractal dimension on the skeletonized images was assessed using the Fractal Box Count function.

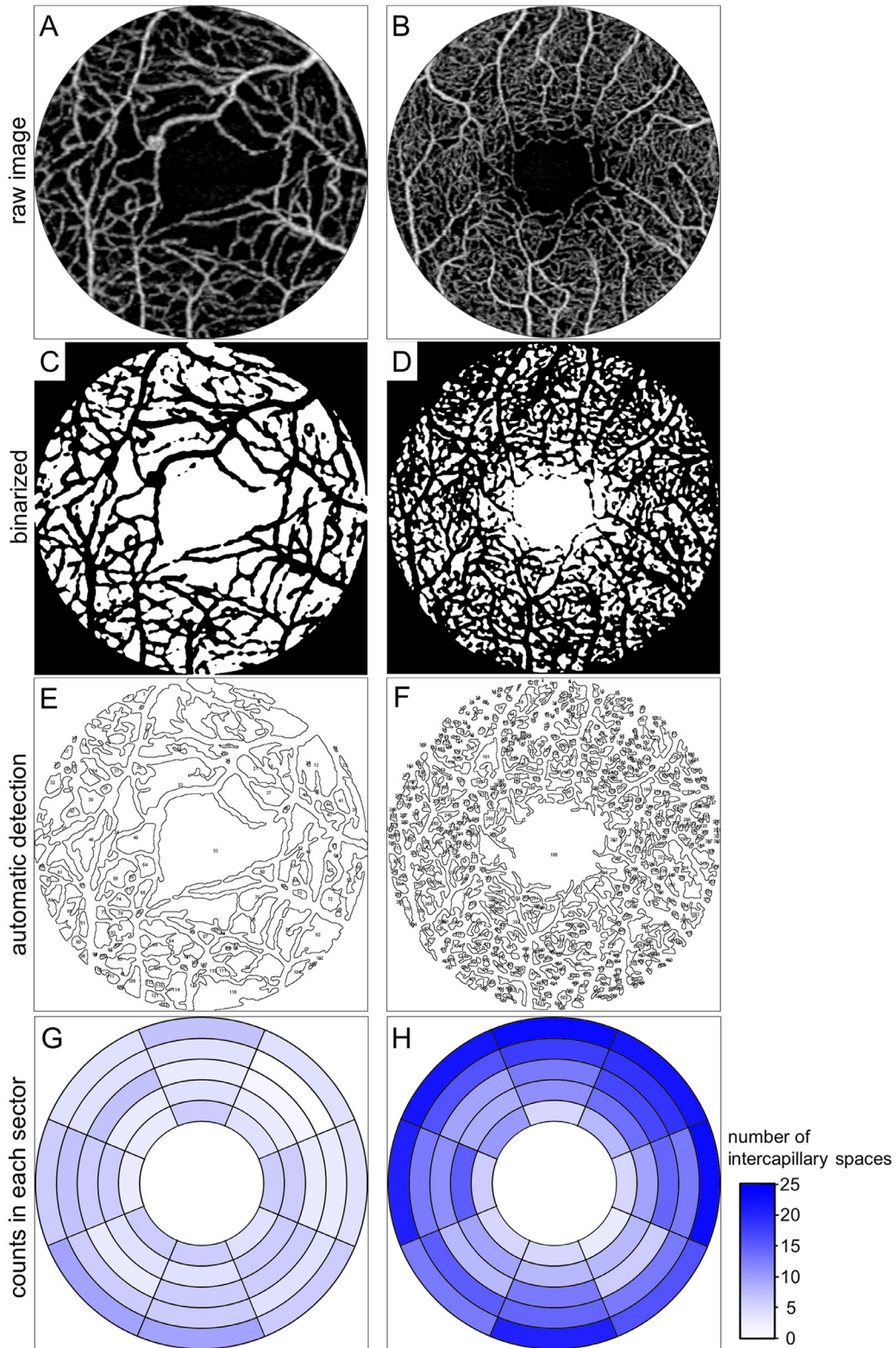


**FIGURE 1.** Automatic quantification of intercapillary spaces in each sector on swept source OCTA images in two representative eyes with DR. (A, C, E, G) The decrease in the number of intercapillary spaces in a 42-year-old man with diabetic macular ischemia and PDR. (B, D, F, H) Abundant intercapillary spaces in a 52-year-old man with severe nonproliferative diabetic retinopathy (NPDR). (A, B) Raw OCTA images of the superficial slab within the central 2-mm circle. (C, D) Binary image (white = intercapillary spaces). (E, F) The intercapillary spaces are detected automatically. (G, H) Pseudocolor maps of the number of intercapillary spaces in each parafoveal sector.



## Statistical Analyses

Results are presented as the median (interquartile range). The Mann–Whitney *U* test or Kruskal–Wallis test with the Bonferroni correction was used for comparisons between groups. Fisher's exact test or the  $\chi^2$  test was applied to test the sampling distribution. Spearman's rank correlation coefficient was used to assess the association between two variables. Particularly, we defined the sector with the best correlations between the number of intercapillary spaces and logMAR ( $\rho < -0.45$ ) as a highly significant sector. The numbers of intercapillary spaces in these sectors were summed to evaluate the relation to logMAR. The sector with a  $\rho$  of less than  $-0.4$  was defined as a significant sector and underwent the similar analyses. We used multivariate analyses to adjust for confounding factors. The significant independent factors ( $P < 0.10$  in univariate analyses) were applied to multivariate regression analysis.

Cluster analyses were performed using Ward's method of dendrogram hierarchical clustering after the normalization of the parameters. We selected two parameters, that is, the FAZ area and total counts of intercapillary spaces and calculated the Euclid distances between two hypothesized clusters. The agglomeration of clusters with the minimal distance was selected. These processes were repeated, and all eyes reached to one cluster. Two major clusters were referred to as the nonperfusion group and the perfusion group. Two minor clusters in the nonperfusion group were as the severe subgroup and the mild subgroup. A *P* value of less than 0.05 was considered statistically significant. These statistical analyses were performed using commercial software (PASW Statistics, version 22; SPSS Inc., Chicago, IL).

## RESULTS

### Relation Between logMAR and Parameters of Intercapillary Space

We investigated the relationship between logMAR and nonperfusion parameters in the macula in 110 eyes of 110 patients with DR without DME. The patients' characteristics are shown in Table 1. We first evaluated the parameters of the automatically defined FAZ. The area, minimum diameter, maximum diameter, and perimeter of the FAZ were related to logMAR (Supplementary Table S1).

TABLE 1. Patient Characteristics

Variables	
Age (years)	62 (50 to 71)
Gender (male/female)	74/36
Hemoglobin A1c (%)	7.4 (6.9 to 8.4)
Duration of diabetes (years)	16 (9 to 23)
Systemic hypertension (present/absent)	61/49
Dyslipidemia (present/absent)	52/58
LogMAR	0.000 (−0.079 to 0.046)
Phakia/pseudophakia	63/47
International DR severity grade (eyes)	
Mild NPDR	9
Moderate NPDR	41
Severe NPDR	12
PDR	48
Prior panretinal photocoagulation (eyes)	46

Values are median (interquartile range) or number.

We further introduced the quantitative parameters of parafoveal intercapillary spaces in this study. Their counts were significantly related to the vessel density, vessel length density, and fractal dimension (Supplementary Fig. S1). The mean area, minimum diameter, maximum diameter, and perimeter of the intercapillary spaces also showed a modest correlation with logMAR (Supplementary Table S1). The total counts of intercapillary spaces were more significantly associated with logMAR than other parameters ( $\rho = -0.419$ ;  $P < 0.001$ ) (Fig. 2A). Other perfusion indices had the similar association with logMAR (Supplementary Fig. S2). In 104 eyes with good vision (logMAR  $< 0.5$ ), the logMAR was more significantly associated with total counts of intercapillary spaces ( $\rho = -0.338$ ;  $P < 0.001$ ) than with the vessel density ( $\rho = -0.308$ ;  $P < 0.001$ ).

We considered additional analyses regarding the size thresholding and the location of intercapillary spaces. We counted the intercapillary spaces with areas smaller than several thresholds, but failed to find more significant associations with logMAR (Supplementary Table S2). In contrast, the counts in three parafoveal sectors, that is, the third ( $\rho = -0.485$ ;  $P < 0.001$ ) and fourth ( $\rho = -0.473$ ;  $P < 0.001$ ) rings of the superotemporal octant and the fourth ring of the superior octant ( $\rho = -0.474$ ;  $P < 0.001$ ) were more significantly associated with logMAR (Fig. 2B). The summed counts in these three highly significant sectors were best related to logMAR ( $\rho = -0.515$ ;  $P < 0.001$ ) (Fig. 2C). We further summed the numbers in seven significant sectors, which showed better correlation with the logMAR ( $\rho = -0.504$ ;  $P < 0.001$ ; Fig. 2D). Additional analyses using other two annulus patterns confirmed the similar trends; the outer or superior sectors had a better association with the logMAR (Supplementary Fig. S3).

We used the multivariate regression analysis to adjust for confounding factors, and revealed that the number of intercapillary spaces in three highly significant sectors and the FAZ area were related to the logMAR (Table 2).

### Cluster Analysis Using Parafoveal Intercapillary Spaces and FAZ

We evaluated the association between the FAZ area and the total counts of intercapillary spaces and found a significant association between them (Fig. 3B). It was strange that no eyes with many intercapillary spaces had an enlarged FAZ, whereas several eyes with fewer intercapillary spaces had a smaller FAZ. Similarly, no eyes with a greater FAZ area were accompanied by smaller mean areas of intercapillary spaces (Fig. 3C). This result suggests a unique trait of diabetic macular ischemia. We, therefore, applied the cluster analysis to evaluate their diagnostic significance in diabetic macular ischemia (Fig. 3A). Agglomerative clustering objectively reached to 2 major groups, which prompted us to define 82 eyes of the first cluster with fewer intercapillary spaces as the nonperfusion group (Table 3). Eyes of the nonperfusion group had poorer logMAR than those of the perfusion group (0.000 [−0.079 to 0.097] vs. −0.079 [−0.176 to 0.011];  $P < 0.001$ ). Multivariate analysis confirmed the association between logMAR and the number of intercapillary spaces in the highly significant sectors in 82 eyes of the nonperfusion group (Supplementary Table S3).

The cluster analysis also revealed two minor clusters; severe subgroup and mild subgroup (Figs. 3A, D). These clusters had the differences in some FAZ parameters and

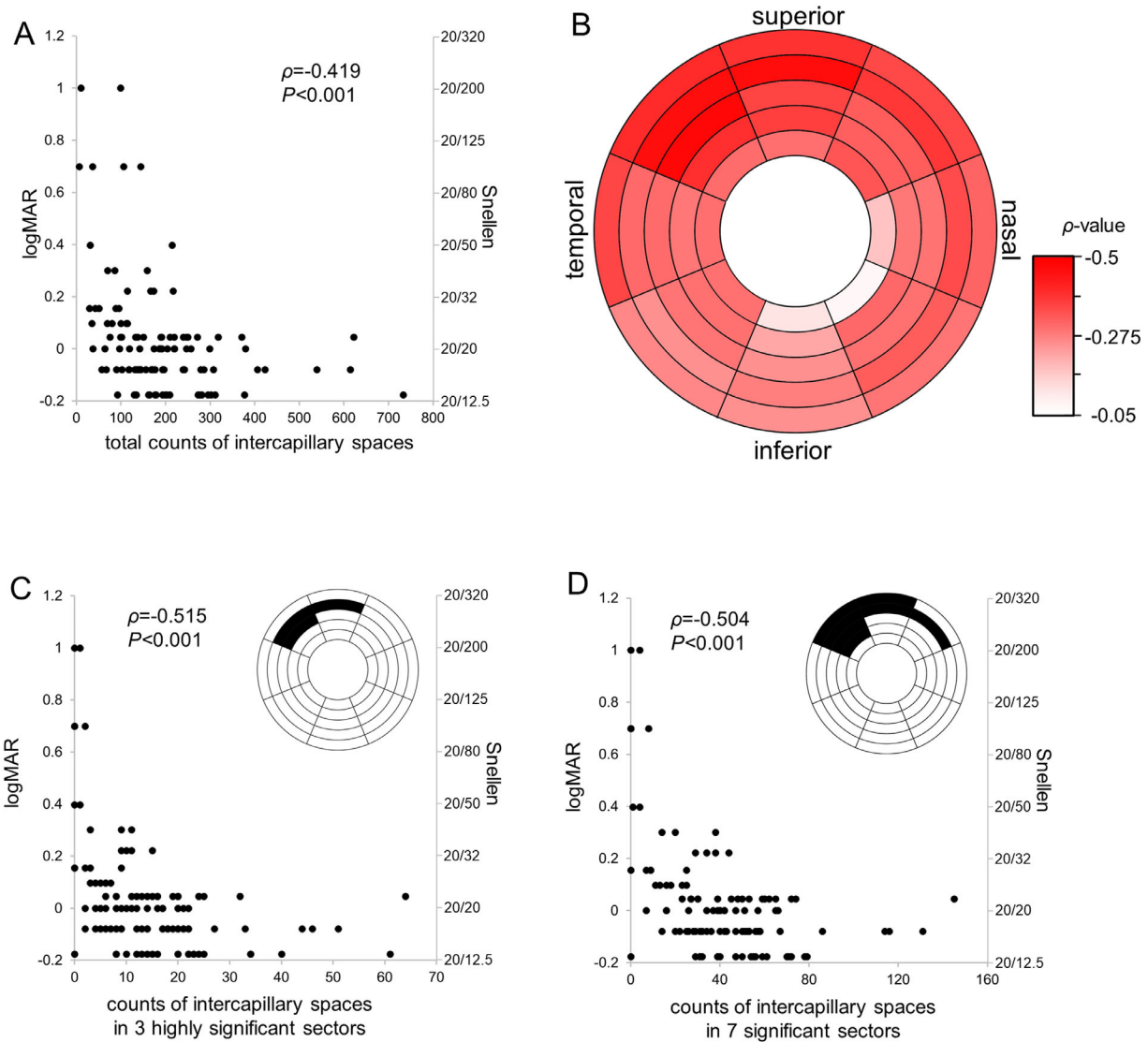


**FIGURE 2.** The association between logMAR and counts of the intercapillary spaces in DR without DME. The significant associations of logMAR with total counts (A), those in three highly significant sectors (C), and those in seven significant sectors (D) of intercapillary spaces. (B) A pseudocolor map of the correlation between logMAR and the number of intercapillary spaces in each sector.

**TABLE 2.** Association of Systemic and Ocular Parameters With logMAR in 110 Eyes With DR

Variables	Univariate			Multivariate		
	Unstandardized $\beta$	Standardized $\beta$	<i>P</i> Value	Unstandardized $\beta$	Standardized $\beta$	<i>P</i> Value
Age (years)	0.001	0.087	0.367	–	–	–
Gender (male)	–0.027	–0.056	0.558	–	–	–
Hemoglobin A1c (%)	–0.009	–0.064	0.527	–	–	–
Duration of diabetes (years)	–0.003	–0.131	0.218	–	–	–
Systemic hypertension	0.011	0.023	0.808	–	–	–
Dyslipidemia	–0.078	–0.171	0.074	–0.043	–0.124	0.160
Pseudophakia	0.077	0.169	0.078	0.007	0.019	0.832
PDR	–0.025	–0.056	0.564	–	–	–
FAZ area (mm <sup>2</sup> )	0.168	0.403	<0.001	0.095	0.227	0.042
No. of intercapillary spaces in the highly significant sectors	–0.003	–0.437	<0.001	–0.002	–0.266	0.016
Prior panretinal photocoagulation	0.144	0.312	0.001	0.040	0.112	0.225

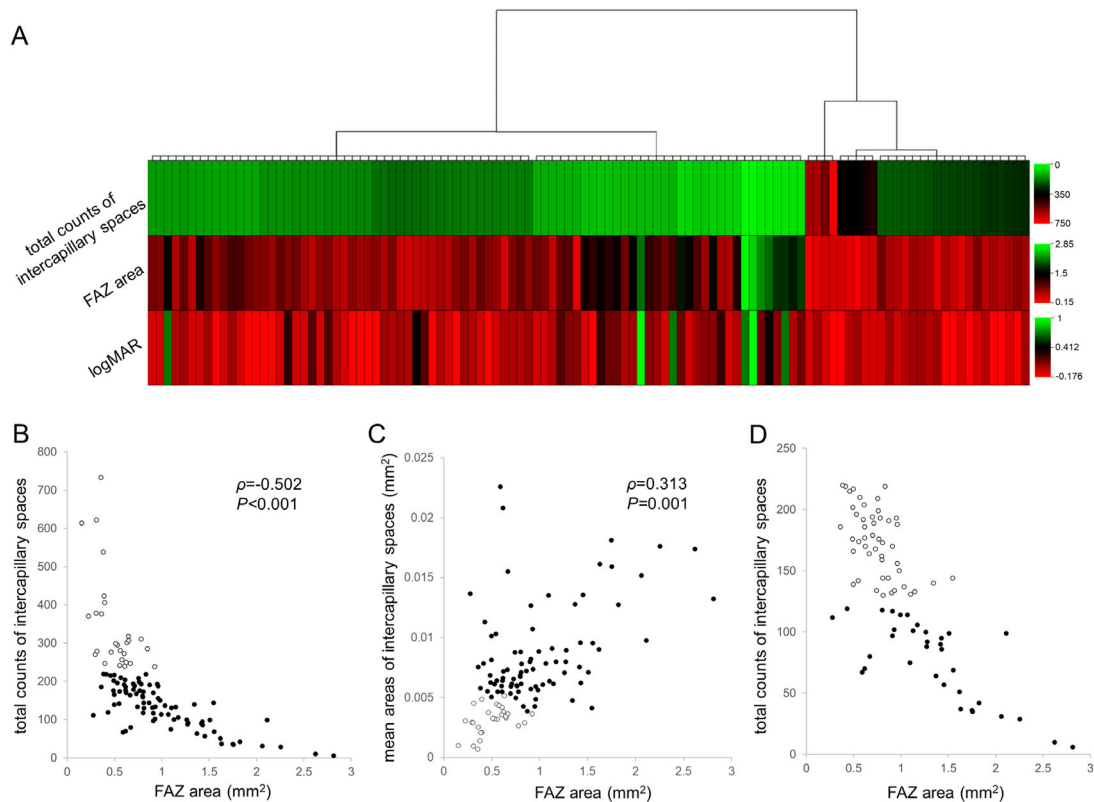


**FIGURE 3.** The clustering using the FAZ area and the total counts of intercapillary spaces discriminates the nonperfusion group from the perfusion group. **(A)** A heatmap of the agglomerative clustering using Ward's method reveals two major clusters. The characteristics of the left cluster represent the nonperfusion group. **(B)** These two clusters (white dots = eyes in the right cluster in **A**; black dots = eyes in the left cluster) are divided by the threshold of the intercapillary spaces (number = 230), but not by the FAZ area, in the scatter plot. **(C)** The scatter plot shows that no eyes with an enlarged FAZ have small mean areas of the intercapillary spaces. **(D)** Two minor clusters in the nonperfusion group. White and black dots correspond with left and right subclusters, respectively.

total counts of intercapillary spaces, but not in DR severity (Supplementary Table S4).

## DISCUSSION

In the current study, we revealed, for the first time, that the number of the intercapillary spaces on OCTA images was negatively associated with logMAR in DR without center-involved DME. This finding suggests that parafoveal ischemic changes in the superficial vascular layer have impacts on VA. Bipolar cells and subsequent ganglion cells from cone photoreceptors are centrifugally displaced, and anatomically correspond with the FAZ and the superficial vascular layer in the parafovea, respectively. Diabetes leads to damages in both capillaries and might contribute to the impairment in ganglion cells and resultant VA decrease, at least in part. Additionally, the clustering using the FAZ and the intercapillary spaces divided 110 eyes into 2 major groups, and further prospective studies should elucidate its clinical feasibility in the objective diagnosis of diabetic macular ischemia.

The FAZ parameters are feasible on both FA and OCTA images, although the parameter of this single finding may be vulnerable to several lines of artifacts in image acquisition, processing, and quantification.<sup>24,25</sup> In addition, the FAZ areas vary in healthy individuals.<sup>26,27</sup> These concerns do not allow us to define the normal value of the FAZ

parameters.<sup>28</sup> In contrast, the parameters of intercapillary spaces can be calculated using many spaces, independent of the inborn morphologic features of the FAZ. Both transient and permanent obstruction of retinal vessels influences flow signals on OCTA images, whereas the transient nonperfusion cannot be observed on FA images.<sup>5,29</sup> Because even the minimal and transient loss of flow signal between intercapillary spaces also makes them fused into one on OCTA images, their morphological parameters increase and their counts decreases in the parafovea. It suggests that such assessment has a high sensitivity for microcirculation impairment. We, therefore, focused on the clinical relevance of the intercapillary spaces compared with those of the FAZ.<sup>17–21</sup>

Among several parameters of intercapillary spaces, their counts showed the most significant correlation to logMAR. As in the case of perfusion metrics, for example, vascular density and its morphologic parameters, the geometric parameters of intercapillary spaces are modulated by vascular morphologic changes, for example, microaneurysms and capillary tortuosity or dilatation. In contrast, the number of intercapillary spaces may depend on vascular obstruction but not on its morphology. We, therefore, speculated that the deficiency of oxygen and nutrients rather than vascular morphologies is one of several factors impairing visual function in DR without DME.<sup>30</sup>

We further investigated the clinically significant sectors and found that the counts of intercapillary spaces in seven

TABLE 3. Characteristics of Eyes in the Nonperfusion and Perfusion Groups

Variables	Nonperfusion Group (82 Eyes)	Perfusion Group (28 Eyes)	P Value
Age (years)	60 (49 to 72)	63 (56 to 69)	0.299
Gender (male/female)	61/21	13/15	0.010
Hemoglobin A1c (%)	7.7 (6.8 to 8.4)	7.2 (6.9 to 8.0)	0.901
Duration of diabetes (years)	16 (10 to 22)	17 (8 to 25)	0.857
Systemic hypertension	49	12	0.130
Dyslipidemia	40	12	0.664
LogMAR	0.000 (−0.079 to 0.097)	−0.079 (−0.176 to 0.011)	<0.001
Phakia/pseudophakia	42/40	21/7	0.045
International DR severity scale			
Mild NPDR	4	5	
Moderate NPDR	26	15	
Severe NPDR	9	3	
PDR	43	5	0.005
FAZ			
Area (10 <sup>−3</sup> mm <sup>2</sup> )	805 (611 to 1196)	567 (386 to 737)	<0.001
Minimum diameter (10 <sup>−1</sup> mm)	12.01 (9.63 to 14.46)	8.76 (6.96 to 10.09)	<0.001
Maximum diameter (10 <sup>−1</sup> mm)	16.38 (14.40 to 19.06)	11.43 (9.31 to 12.44)	<0.001
Perimeter (10 <sup>−1</sup> mm)	186.5 (119.5 to 237.2)	94.2 (54.2 to 122.7)	<0.001
Intercapillary spaces			
Total counts	138 (96 to 179)	297 (268 to 378)	<0.001
Mean area (10 <sup>−3</sup> mm <sup>2</sup> )	7.15 (5.96 to 9.00)	3.23 (2.60 to 3.76)	<0.001
Mean minimum diameter (10 <sup>−1</sup> mm)	0.613 (0.565 to 0.687)	0.433 (0.398 to 0.470)	<0.001
Mean maximum diameter (10 <sup>−1</sup> mm)	1.213 (1.063 to 1.361)	0.878 (0.787 to 0.952)	<0.001
Mean perimeter (10 <sup>−1</sup> mm)	4.24 (3.63 to 5.10)	2.57 (2.29 to 3.02)	<0.001
Prior panretinal photocoagulation	42	4	<0.001

Values are median (interquartile range) or number.

significant sectors were feasible to infer VA reduction in DR. The numbers of intercapillary spaces in several sectors in the outer rings were significantly associated with VA reduction. Anatomically, ganglion cells or their axons from foveal photoreceptors reside in the outer ring, because bipolar and ganglion cells are centrifugally displaced in the macula.<sup>14</sup> The correspondence between structure OCT and OCTA revealed the damages in ganglion cells in the NPAs in the superficial layer.<sup>11</sup> Histological publications also confirmed the degenerative changes in ganglion cells in diabetic retinas.<sup>31,32</sup> We, therefore, hypothesized that the capillary nonperfusion promotes ganglion cell impairment or vice versa. Retinal ganglion cells, in which action potentials are elicited, consume a large amount of adenosine triphosphate to keep resting membrane potential and repolarization.<sup>30</sup> They are far from the choroid and nourished only by the retinal vessels, compared with the bipolar cells and photoreceptors. The disturbed blood flow in the superficial capillaries of the parafovea may decrease the supply of oxygen and glucose to retinal ganglion cells. Adenosine triphosphate depletion would impair the function or promote the degeneration in the ganglion cells. Inversely, diabetes initially induces neurodegeneration in the retinas, especially in the ganglion cells, mediated via several mechanisms. Loss of ganglion cells may decrease VEGF secretion and promote capillary dropout.<sup>33,34</sup>

All significant sectors, in which capillary nonperfusion was highly associated with VA reduction, were located in the superior hemifield rather than in the inferior hemifield. Major previous publications demonstrated that the retinas in the superior quadrant tend to have greater thicknesses on OCT imaging and higher perfusion metrics in the superficial OCTA images than those in the inferior quadrant in healthy eyes.<sup>35,36</sup> This finding suggests that retinal parenchyma in the superior areas needs greater amounts of oxygen and

glucose, which are supplied by denser capillaries. In addition, the inner retinal layers of the superior areas are farther from the choroidal nourishment. In contrast, there were no differences in the capillary flow density between the superior and inferior quadrant in diabetic eyes.<sup>37</sup> These publications may allow us to speculate that capillary nonperfusion in the superficial layer promotes ganglion cell dysfunction more significantly in the superior hemifield than in the inferior hemifield.

Multivariate analyses showed that poor VA was associated with the reduced counts of intercapillary spaces in all 110 eyes with DR, compared with the marginal association with the FAZ area. Surprisingly, statistical analyses in 82 eyes of the nonperfusion group suggested that the FAZ is a confounding factor. Bipolar cells, which correspond with the FAZ, might be tolerant of microcirculatory disturbance in the retina, and choroidal vessels might nourish them via Müller cells and retinal pigment epithelium at least partly.

We evaluated the relationship between the FAZ area and the number of intercapillary spaces. There were no eyes with an enlarged FAZ and a normal level of intercapillary spaces, although the FAZ is surrounded by the most distal capillaries. No eyes had both an enlarged FAZ and a higher density of intercapillary spaces outside the FAZ (data not shown). The artery–capillary–vein unit in the superficial vascular plexus of the parafovea may not allow the redundant perfusion and promote the propagation of capillary obstruction.<sup>38</sup> In contrast, several arteries are connected to the perifoveal capillary network, and deep vascular plexuses may serve as the collateral vessels to it.<sup>6,39</sup>

Despite its clinical significance, there is no consensus regarding the definition of diabetic macular ischemia.<sup>13,21,40,41</sup> Several perfusion or nonperfusion indices are candidates for diagnostic criteria. We considered that diagnostic parameters should be associated with



visual impairment and have definite thresholds to discriminate eyes with the disease from those with no disease. Among nonperfusion indices, the counts of intercapillary spaces may be one of the candidates for the objective and quantitative diagnosis of diabetic macular ischemia. The counts were more significantly associated with logMAR than the morphological parameters in the FAZ and intercapillary spaces. Additionally, we could not find the definite thresholds in the mean areas for the diagnosis of diabetic macular ischemia (Fig. 3C). The comparative study suggests that the counts of intercapillary spaces are feasible for the early diagnosis and the vessel density is useful for the grading in the severe cases. Future prospective studies should determine better metrics for the diagnosis.<sup>42–44</sup>

There are several limitations in this single-center, retrospective study. Although we reviewed consecutive cases, several inclusion and exclusion criteria may result in selection bias. In particular, we could not include eyes with severe VA reduction and poor fixation, because the OCTA machine used in this study did not delineate images with sufficient quality in such eyes. The media opacity would affect the quality of flow signals on OCTA images and might lead to the minor errors in further analyses. Although we carefully excluded eyes with severe segmentation error, the segmentation may influence the delineation of superficial retinal vessels. This image processing could not detect intercapillary spaces in the deep capillary plexus and did not allow us to evaluate them. The quantification of intercapillary spaces may depend on the machine used for image acquisition and the algorithm used for the automatic detection of intercapillary spaces. Multiple tests for statistical associations might lead to false-positive results, and the confounders might influence the statistical results. Future longitudinal and multicenter studies should confirm the reproducibility of other OCTA machines and other image processing algorithms in other populations.

In the current study, we demonstrated, for the first time, that the intercapillary spaces in the parafoveal and superficial vascular plexuses have significant impacts on logMAR in DR without DME. The clustering using parafoveal intercapillary spaces and the FAZ discriminated the nonperfusion group from the perfusion group, that suggests that they are candidates for the objective and quantitative diagnostic criteria of diabetic macular ischemia.

### Acknowledgments

Supported by a Grant-in-Aid for Scientific Research of the Japan Society for the Promotion of Science (Grant Number: 20K09788). The funding organization had no role in the design or conduct of this research.

Disclosure: N. Terada, None; T. Murakami, None; K. Ishihara, None; Y. Dodo, None; K. Nishikawa, None; K. Kawai, None; A. Tsujikawa, None

### References

- Antonetti DA, Klein R, Gardner TW. Diabetic retinopathy. *N Engl J Med*. 2012;366(13):1227–1239.
- Yau JW, Rogers SL, Kawasaki R, et al. Global prevalence and major risk factors of diabetic retinopathy. *Diabetes Care*. 2012;35(3):556–564.
- Dodo Y, Murakami T, Uji A, Yoshitake S, Yoshimura N. Disorganized retinal lamellar structures in nonperfused areas of diabetic retinopathy. *Invest Ophthalmol Vis Sci*. 2015;56(3):2012–2020.
- Sun JK, Lin MM, Lammer J, et al. Disorganization of the retinal inner layers as a predictor of visual acuity in eyes with center-involved diabetic macular edema. *JAMA Ophthalmol*. 2014;132(11):1309–1316.
- Cheung CMG, Fawzi A, Teo KY, et al. Diabetic macular ischaemia—a new therapeutic target? *Prog Retin Eye Res*. 2021;101033.
- Snodderly DM, Weinhaus RS, Choi JC. Neural-vascular relationships in central retina of macaque monkeys (*Macaca fascicularis*). *J Neurosci*. 1992;12(4):1169–1193.
- Classification of diabetic retinopathy from fluorescein angiograms. ETDRS report number 11. Early Treatment Diabetic Retinopathy Study Research Group. *Ophthalmology*. 1991;98(5 Suppl):807–822.
- Jia Y, Tan O, Tokayer J, et al. Split-spectrum amplitude-decorrelation angiography with optical coherence tomography. *Opt Express*. 2012;20(4):4710–4725.
- Spaide RF, Klancnik JM, Cooney MJ. Retinal vascular layers imaged by fluorescein angiography and optical coherence tomography angiography. *JAMA Ophthalmol*. 2015;133(1):45–50.
- Byeon SH, Chu YK, Lee H, Lee SY, Kwon OW. Foveal ganglion cell layer damage in ischemic diabetic maculopathy: correlation of optical coherence tomographic and anatomic changes. *Ophthalmology*. 2009;116(10):1949–1959.e1948.
- Dodo Y, Murakami T, Suzuma K, et al. Diabetic neuroglial changes in the superficial and deep nonperfused areas on optical coherence tomography angiography. *Invest Ophthalmol Vis Sci*. 2017;58(13):5870–5879.
- Balaratnasingam C, Inoue M, Ahn S, et al. Visual acuity is correlated with the area of the foveal avascular zone in diabetic retinopathy and retinal vein occlusion. *Ophthalmology*. 2016;123(11):2352–2367.
- Samara WA, Shahlaee A, Adam MK, et al. Quantification of diabetic macular ischemia using optical coherence tomography angiography and its relationship with visual acuity. *Ophthalmology*. 2017;124(2):235–244.
- Sjostrand J, Popovic Z, Conradi N, Marshall J. Morphometric study of the displacement of retinal ganglion cells subserving cones within the human fovea. *Graefes Arch Clin Exp Ophthalmol*. 1999;37(12):1014–1023.
- Terada N, Murakami T, Uji A, et al. The intercapillary space spectrum as a marker of diabetic retinopathy severity on optical coherence tomography angiography. *Sci Rep*. 2022;12(1):3089.
- Chalam KV, Bressler SB, Edwards AR, et al. Retinal thickness in people with diabetes and minimal or no diabetic retinopathy: Heidelberg Spectralis optical coherence tomography. *Invest Ophthalmol Vis Sci*. 2012;53(13):8154–8161.
- Schottenhamml J, Moulton EM, Ploner S, et al. An automatic, intercapillary area-based algorithm for quantifying diabetes-related capillary dropout using optical coherence tomography angiography. *Retina*. 2016;36(Suppl 1):S93–S101.
- Krawitz BD, Phillips E, Bavier RD, et al. Parafoveal nonperfusion analysis in diabetic retinopathy using optical coherence tomography angiography. *Transl Vis Sci Technol*. 2018;7(4):4.
- Lauermann P, van Oterendorp C, Storch MW, et al. Distance-thresholded intercapillary area analysis versus vessel-based approaches to quantify retinal ischemia in OCTA. *Transl Vis Sci Technol*. 2019;8(4):28.
- Alibhai AY, De Pretto LR, Moulton EM, et al. Quantification of retinal capillary nonperfusion in diabetics using wide-field optical coherence tomography angiography. *Retina*. 2020;40(3):412–420.



21. Borrelli E, Sacconi R, Querques L, Battista M, Bandello F, Querques G. Quantification of diabetic macular ischemia using novel three-dimensional optical coherence tomography angiography metrics. *J Biophotonics*. 2020;13(10):e202000152.
22. Bennett AG, Rudnicka AR, Edgar DF. Improvements on Littmann's method of determining the size of retinal features by fundus photography. *Graefes Arch Clin Exp Ophthalmol*. 1994;32(6):361–367.
23. Kawai K, Murakami T, Sakaguchi S, et al. Peripheral chorioretinal imaging through a front prism on optical coherence tomography angiography. *Transl Vis Sci Technol*. 2021;10(14):36.
24. Ghasemi Falavarjani K, Al-Sheikh M, Akil H, Sadda SR. Image artefacts in swept-source optical coherence tomography angiography. *Br J Ophthalmol*. 2017;101(5):564–568.
25. Spaide RF, Fujimoto JG, Waheed NK. Image artifacts in optical coherence tomography angiography. *Retina*. 2015;35(11):2163–2180.
26. Bowl W, Bowl M, Schweinfurth S, et al. OCT angiography in young children with a history of retinopathy of prematurity. *Ophthalmol Retina*. 2018;2(9):972–978.
27. Mintz-Hittner HA, Knight-Nanan DM, Satriano DR, Kretzer FL. A small foveal avascular zone may be an historic mark of prematurity. *Ophthalmology*. 1999;106(7):1409–1413.
28. Takase N, Nozaki M, Kato A, Ozeki H, Yoshida M, Ogura Y. Enlargement of foveal avascular zone in diabetic eyes evaluated by en face optical coherence tomography angiography. *Retina*. 2015;35(11):2377–2383.
29. Spaide RF, Fujimoto JG, Waheed NK, Sadda SR, Staurengi G. Optical coherence tomography angiography. *Prog Retin Eye Res*. 2018;64:1–55.
30. Pournaras CJ, Rungger-Brandle E, Riva CE, Hardarson SH, Stefansson E. Regulation of retinal blood flow in health and disease. *Prog Retin Eye Res*. 2008;27(3):284–330.
31. Barber AJ, Lieth E, Khin SA, Antonetti DA, Buchanan AG, Gardner TW. Neural apoptosis in the retina during experimental and human diabetes. Early onset and effect of insulin. *J Clin Invest*. 1998;102(4):783–791.
32. Kern TS, Barber AJ. Retinal ganglion cells in diabetes. *J Physiol*. 2008;586(18):4401–4408.
33. Kim I, Ryan AM, Rohan R, et al. Constitutive expression of VEGF, VEGFR-1, and VEGFR-2 in normal eyes. *Invest Ophthalmol Vis Sci*. 1999;40(9):2115–2121.
34. Lee S, Chen TT, Barber CL, et al. Autocrine VEGF signaling is required for vascular homeostasis. *Cell*. 2007;130(4):691–703.
35. Grover S, Murthy RK, Brar VS, Chalam KV. Normative data for macular thickness by high-definition spectral-domain optical coherence tomography (Spectralis). *Am J Ophthalmol*. 2009;148(2):266–271.
36. You QS, Chan JCH, Ng ALK, et al. Macular vessel density measured with optical coherence tomography angiography and its associations in a large population-based study. *Invest Ophthalmol Vis Sci*. 2019;60(14):4830–4837.
37. Kaizu Y, Nakao S, Yoshida S, et al. Optical coherence tomography angiography reveals spatial bias of macular capillary dropout in diabetic retinopathy. *Invest Ophthalmol Vis Sci*. 2017;58(11):4889–4897.
38. Chan G, Balaratnasingam C, Yu PK, et al. Quantitative morphometry of perifoveal capillary networks in the human retina. *Invest Ophthalmol Vis Sci*. 2012;53(9):5502–5514.
39. Nesper PL, Fawzi AA. Human parafoveal capillary vascular anatomy and connectivity revealed by optical coherence tomography angiography. *Invest Ophthalmol Vis Sci*. 2018;59(10):3858–3867.
40. Scarinci F, Nesper PL, Fawzi AA. Deep retinal capillary nonperfusion is associated with photoreceptor disruption in diabetic macular ischemia. *Am J Ophthalmol*. 2016;168:129–138.
41. Tsai ASH, Gan ATL, Ting DSW, et al. Diabetic macular ischemia: correlation of retinal vasculature changes by optical coherence tomography angiography and functional deficit. *Retina*. 2020;40(11):2184–2190.
42. Agemy SA, Sripsema NK, Shah CM, et al. Retinal vascular perfusion density mapping using optical coherence tomography angiography in normals and diabetic retinopathy patients. *Retina*. 2015;35(11):2353–2363.
43. Rosen RB, Andrade Romo JS, Krawitz BD, et al. Earliest evidence of preclinical diabetic retinopathy revealed using optical coherence tomography angiography perfused capillary density. *Am J Ophthalmol*. 2019;203:103–115.
44. Zahid S, Dolz-Marco R, Freund KB, et al. Fractal dimensional analysis of optical coherence tomography angiography in eyes with diabetic retinopathy. *Invest Ophthalmol Vis Sci*. 2016;57(11):4940–4947.